BBA - Proteins and Proteomics 1869 (2021) 140563

Contents lists available at ScienceDirect

BBA - Proteins and Proteomics

journal homepage: www.elsevier.com/locate/bbapap

Research Paper

Ceruloplasmin and oxidative stress in severe eosinophilic asthma patients treated with Mepolizumab and Benralizumab

Claudia Landi [a,b,1], Paolo Cameli [b,1], Lorenza Vantaggiato [a], Laura Bergantini [b], Miriana d'Alessandro [b], Marco Perruzza [b], Alfonso Carleo [c], Enxhi Shaba [a], Fabrizio Di Giuseppe [d], Stefania Angelucci [d], Elena Bargagli [b,*], Luca Bini [a]

[a] Functional Proteomics Lab, Department of Life Sciences, University of Siena, Siena, Italy
[b] UOC Respiratory Diseases and Lung Transplantation, Department Internal and Specialist Medicine, University of Siena, Siena, Italy
[c] Department of Pulmonology, Hannover Medical School, Hannover, Germany
[d] Dept. Medical, Oral & Biotechnological Sciences, Dentistry and Biotechnology, and Proteomics Unit, Centre of Advanced Studies and Technoloy, "G. d'Annunzio", University of Chieti-Pescara, Italy

ARTICLE INFO

Keywords:
Mepolizumab
Benralizumab
Redox proteomics
Serum
Severe eosinophilic asthma

ABSTRACT

Introduction: Severe eosinophilic asthma has been associated with Th2 airway inflammation and elevated proinflammatory cytokines and chemokines, such as IL-5. Precision therapies have recently been shown to improve asthma symptoms with a steroid-sparing effect. Two such therapies, Benralizumab and Mepolizumab, humanized IgG antibodies directed against the IL-5 receptor and IL-5, have been approved for severe eosinophilic asthma.

Methods: Here we used a differential proteomic approach to analyse serum from patients with severe eosinophilic asthma treated with Benralizumab and Mepolizumab in a search for differential molecular modifications responsible of their effects. Enrichment analysis of differential proteins was performed for the two treatments.

Results and discussion: After one month of Benralizumab treatment we detected up-regulation of certain protein species of the antioxidant ceruloplasmin. To investigate oxidative stress, we performed redox proteomics which detected lower oxidative burst after one month of Benralizumab treatment than in the pre-treatment phase or after one month of Mepolizumab therapy.

1. Introduction

In the last ten years, the scientific community has formulated a new definition of asthma. Asthma is now regarded as a heterogeneous inflammatory disorder with several specific phenotypes ("Global Initiative for the Management of Asthma 2015," 2016). Approximately 5–10% of the 300 million asthmatics worldwide have a severe form [1]. Eosinophilic asthma, a major subtype of asthma associated with increased risk of severe exacerbations and symptoms refractory to high doses of steroids and other conventional therapies, accounts for 40–60% of this population. Severe eosinophilic asthma is also characterized by airway hyper-reactivity, hypereosinophilia in blood and sputum, thickening of the reticular basement membrane and overexpression of Th2 inflammatory cytokines, including IL-5, TGF-β, VEGF, MMP-9, TIMP-1 and IL-13 [1]. Given the crucial role of IL-5 in the recruitment and survival of eosinophils in peripheral tissues, biological drugs targeting this pleiotropic cytokine have been developed in order to regulate eosinophil-mediated inflammation in uncontrolled and symptomatic asthma patients with high eosinophil peripheral count [1].

Mepolizumab is a humanized monoclonal N-glycosylated IgG1/k antibody that binds the IL-5 α- chain, preventing it from connecting with the α subunit of the IL-5 receptor (IL-5R) [2]. Benralizumab differs from Mepolizumab in that it directly targets the IL-5Ra subunit, expressed mainly by eosinophils and basophils. Benralizumab is also known to have a higher affinity for human FcγRIIIa, resulting in enhanced antibody-dependent cellular cytotoxicity ADCC action [3], and consequently in a reduction in circulating levels of eosinophils and basophils [4]. Mepolizumab [5–10] and Benralizumab [11–14] are reliably

* Corresponding author: UOC Respiratory Diseases and Lung Transplantation, Department Internal and Specialist Medicine, University of Siena, Viale Bracci 16, 53100, SI, Italy.
E-mail address: bargagli2@unisi.it (E. Bargagli).
[1] These authors contributed equally to this work.

https://doi.org/10.1016/j.bbapap.2020.140563
Received 16 July 2020; Received in revised form 16 October 2020; Accepted 5 November 2020
Available online 8 November 2020
1570-9639/© 2020 Elsevier B.V. All rights reserved.

effective in reducing asthma exacerbations, steroid requirements and eosinophil peripheral count, and in improving quality of life and lung function parameters. However, biological therapies inevitably raise the question of the one best suited to a specific patient, in line with a "precision medicine" approach. Other aspects in need of clarification are the response to these new drugs, the optimal duration of treatment, persistence of effectiveness and safety. In this scenario, the identification of biomarkers which could help clinicians choose treatment according to biological evidence, is a stimulating challenge for asthma research [15,16,45].

Here we compared the serum proteomic profiles of patients with severe asthma, before (T0) and after one month of Mepolizumab (T1M) and Benralizumab (T1B) therapy for insights into drug-induced molecular modifications.

2. Materials and methods

2.1. Population

Eighteen adult Caucasian patients with severe eosinophilic asthma, treated with anti-IL-5 biological therapy, were enrolled in the study. Ten patients were treated with Mepolizumab and eight with Benralizumab. All patients were monitored at Siena University Regional Referral Centre for Rare Lung Diseases. Severe eosinophilic asthma was diagnosed according to international guidelines, as previously reported [17]. The doses were Mepolizumab subcutaneous 100 mg every 4 weeks and Benralizumanb subcutaneous 30 mg every 4 weeks. Clinical, functional and immunological data was entered in an electronic database.

Serum samples were collected from healthy volunteers (2 males, 2 females, age 45 ± 12, all non-smokers: control group) for evaluation of ceruloplasmin. Controls had no history of respiratory diseases or allergies and were not on any medication at the time of serum sampling. Patients and controls gave their written informed consent to participation in the study, which was approved by our Local Ethics Committee (OSS_REOS code number 12908).

2.2. Lung function tests

Lung function tests were performed at baseline and after one month of therapy for all patients. The following lung function measurements were recorded according to standard ATS/ERS criteria using a Jaeger body plethysmograph with corrections for temperature and barometric pressure: forced expiratory volume in the first second (FEV1), forced vital capacity (FVC) and FEV1/FVC ratio. FEV1 and FVC were expressed in ml and percentage of predicted values.

2.3. Serum preparation for 2DE analysis

Blood was collected in the morning, after 8 h of fasting, directly into serum tubes (BD vacutainer, SST II Advance, Plymouth UK) and centrifuged for 10 min at 1690 x*g*. The serum was recovered and stored at −80 °C until analysis. For proteomic analysis, 10 μl serum was diluted in 16 μl denaturing buffer (10% SDS *w/v* and 2.3% DTE *w/v*) and then heated to 95 °C for 7 min. Lysis buffer containing 8 M UREA w/v, 4% CHAPS w/v, 1% DTE w/v was added to a final volume of 500 μl. {Citation} Fifty microliters of this prepared sample contained 60 μg proteins and was cup-loaded on IPGstrips for the analytical run. 120 μg proteins were cup-loaded for 2D western blot and 600 μg proteins were used for the mass spectrometry preparatory run. Every serum sample was resolved independently by 2DE.

2.4. Two-dimensional electrophoresis and image analysis

Isoelectric focusing was performed using the Immobiline–polyacrylamide system as described [18,19]. It was carried out with a non-linear wide-range immobilized pH gradient (pH 3–10; 18 cm long IPG strips; GE Healthcare, Uppsala, Sweden) using an Ettan™ IPGphor™ system (GE Healthcare). IPG strips were rehydrated with 350 μl lysis buffer and 0.2% (*v*/v) carrier ampholyte for analytical and transfer runs and 2% (v/v) carrier ampholyte for MS-preparatory runs at room temperature for 12 h. Sample load was then performed by cup-loading on the Ettan IPGphor manifold (GE Healthcare) and the run was performed at 16 °C under the following conditions: 200 V for 8 h, a gradient to 3500 V in 2 h, a step at 3500 V for another 2 h, a gradient to 5000 V in 2 h, maintained at 5000 V for another 3 h, another gradient to 8000 V in 1 h and a step at 8000 V for 3 h. Finally, a gradient to 10,000 V in 1 h and maintenance for a total of 100,000 Vh. After the equilibration step [19], the second dimension was carried out on 9–16% polyacrylamide linear-gradient gels. Spot labelling was performed with silver diaminohydroxide solution, as previously described [20,21], while spots on MS-preparatory gels were stained using MS-compatible silver nitrate [22]. Silver stained gels were digitalized using an Image Scanner III laser densitometer and the corresponding LabScan 6.0 software (GE Healthcare). Computer-aided 2D image analysis for spot quantification and comparison, was carried out using Image Master 2D Platinum 7.0 software (GE Healthcare). Ten maps were compared for T0, five for T1M and five for T1B. The obtained gels Masters (T0, T1M, T1B) were then matched together with the Image Master Platinum algorithm to find quantitative and qualitative differences. Differentially abundant spots were considered to be those that differed in mean relative volume (%V) by at least ±1.4-fold between T0, T1M and T1B (Vol: integral of optical density with respect to spot area; %V: Vol of a single spot divided by the total volume of spots computed over the whole image and expressed as a percentage).

Statistical analysis was performed by Kruskall Wallis test ($p \leq 0.05$) and FDR. Significant results were followed by comparisons of mean ranks by Dunn's test using RStudio Desktop 1.1.463 (Integrated Development for RStudio, Inc., Boston, USA, www.rstudio.com). Up-regulated protein distribution between T1B, T0 and T1M was visualized using a three-way Venn diagram with Venny software 2.1 (https://bioinfogp.cnb.csic.es/tools/venny/).

2.5. Identification of differential proteins by mass spectrometry

Spot differences were picked manually and analysed by peptide mass fingerprinting (PMF) with a MALDI-TOF/TOF spectrometer. After protein spot digestion in 50 mM NH_4HCO_3 containing trypsin, incubated overnight at 37 °C, the peptide extract was applied to a C18ZipTip (Millipore, CA, USA), rinsed with a 0.1% TFA and eluted directly on the MALDI target with 0.5 μl saturated α-cyano-4-hydroxycinnamic acid (1:1 = ACN:0.1% TFA) solution. Trypsin digests were analysed with an Autoflex™ Speed mass spectrometer (Bruker Daltonics, Bremen, Germany) equipped with Nd:YAG laser (355 nm; 1000 Hz) operated by FlexControl v3.3 and a 355-nm nitrogen laser. All spectra were obtained by delayed extraction technology in positive reflectron mode and averaged over 100 laser shots to improve the S/N ratio. External high precision calibration was performed using a peptide mixture containing bradykinin (fragment 1–7) 757.39 *m/z*, angiotensin II 1046.54 m/z, ACTH (fragment 18–39) 2465.19 m/z, Glu fibrinopeptide B 1571.57 m/z and renin substrate tetradecapeptide porcine 1760.02 m/z. Samples analysed by PMF were additionally analysed by LIFT MS/MS from the same target. The most abundant ions per sample were chosen for MS/MS

analysis. Analyses were performed in positive LIFT reflectron mode. Precursor ion selector range was 0.65% of parent ion mass. The voltage parameters were set at IS1 6 kV, IS2 5.3 kV, lens 3.00 kV, reflector 1 27.0 kV, reflector 2 11.45 kV, LIFT1 19 kV and LIFT 2 4.40 kV [23].

After MS recording, the spectra underwent PMF, searching the human NCBIn protein database with a Mascot search engine, which compares experimentally-determined tryptic peptide masses with theoretical peptide masses calculated for proteins from these databases. The search parameters were: search type, peptide mass fingerprint enzyme, trypsin; fixed modification, carbamidomethylation (Cys); variable modifications, oxidation of methionine; mass values, monoisotopic. Ion charge state was set at +1; maximum missed cleavages were set at 1; mass tolerance was set at 100 ppm for PMF and 0.6–0.8 Da for MS/MS. After automated assessment of the search results, the samples automatically underwent LIFT TOF/TOF recording for validation of the PMF data analysis. A maximum of four precursor ions per sample was chosen for MS/MS analysis. Protein database searches, *via* Mascot, using combined PMF and MS/MS datasets were performed by BioTools 3.2 (Bruker Daltonics) connected to the Mascot search engine used for SwissProt database search of datasets [24].

2.6. PCA, t-SNE and heat map analysis

Unsupervised matched spots were used to perform multivariate analysis by Principal Component Analysis (PCA) and t-Distributed Stochastic Neighbour Embedding (t-SNE). With PCA it is possible to visualize experimental groups in two dimensions on the basis of spot patterns, simplifying the amount of data (%V variables) by linear transformation. Black lines connect two points representing sera of the same patient before and after therapy. PCA and t-SNE were performed by RStudio Desktop 1.1.463 (Integrated Development for RStudio, Inc., Boston, USA, www.rstudio.com). In particular, unsupervised PCA and unsupervised t-SNE plots were carried out using the %V data of the hundred most differential protein spots according variance in the overall cohort. Another PCA analysis limited to the differentially abundant protein spots corresponding to ceruloplasmin was also carried out.

In order to visualize the abundance of the matched spots in each gel for T0, T1B and T1M, heat map analysis was performed using the %V spot values. Clustering of protein spots was performed on the basis of Euclidean distance. The above analysis and corresponding figures were obtained using RStudio Desktop 1.1.463 (Integrated Development for RStudio, Inc., Boston, USA, https://www.rstudio.com).

2.7. MetaCore analysis

The accession numbers of the specific proteins identified for T1B *vs* T0 and T1M *vs* T0 were entered in MetaCore (Clarivate Analytics, Boston, MA, USA) to obtain correlated protein network and biological processes from the Gene Ontology knowledgebase. MetaCore has a manually annotated database of protein interactions and metabolic reactions from the scientific literature. Since processing used the shortest path algorithm, only proteins known to be closely related were included in the resulting network. Hypothetical networks were built between experimental proteins and the MetaCore protein database. Networks were visualized graphically as nodes (proteins) and edges (links between proteins) and relevant biological processes were then prioritized according to their statistical significance ($p \leq 0.001$ and FDR), reporting the proteins involved in each biological process.

2.8. 1DE and 2DE western blot of ceruloplasmin

For western blot of one-dimensional electrophoresis (1DEWB) against ceruloplasmin, six serum samples for each condition (control, T0, T1M and T1B) were prepared as described above and aliquots of samples were diluted in Laemmli buffer (100 mM Tris–HCl pH 6.8, 2% (*w/v*) SDS, 20% (*v*/v) glycerol, 4% (v/v) β-mercaptoethanol) and heated to 95 °C for five minutes. We loaded 20 μg of proteins for each sample and separated them on 12% polyacrylamide gel. For 2DEWB, we resolved two further samples per condition. After 1DE and 2DE separation, proteins were transferred to a PVDF membrane (Hybond ECL, GE Healthcare) [25]. Ponceau Red staining (0.2% w/v Ponceau S in 3% v/v trichloroacetic acid) of membranes was performed to verify correct protein transfer and to assess equal protein loading. Western blot analysis was performed using mouse monoclonal antibodies against ceruloplasmin 1:1000 (ThermoFisher). The immunoreactive spots were detected using goat peroxidase-conjugated anti-mouse immunoglobulin G (Sigma, working dilution 1:7000) and an ECL chemiluminescence detection system (GE Healthcare). Chemiluminescent signals were captured at different exposure times (20 s, 3 min, 10 min, 20 min). The digital 1D and 2D western blot images were then analysed with Image Master Platinum 7.0 to carry out semi-quantitative analysis using the relative integrated density values of detected spots (spot intensity). Immunoblot data was then exported into Excel (Microsoft Office) to perform *t*-test statistical analysis.

2.9. Redox proteomics

Two serum samples for each condition (T0, T1M and T1B) were resolved by 2DE as described above. After the first run, the strips were derivatized to detect carbonyl groups by rinsing with water and incubating at room temperature in 5% TCA containing 2,4-dinitrophenylhydrazine (DNPH) 10 mM for 20 min. The DNPH-treated strips were washed twice with a solution containing 8 M urea, 20% *v*/v glycerol, 1% *w/v* SDS and 150 mM Tris-HCl (pH 6.8) for 5 min [26] and then equilibrated as described [19]. After equilibration and the second-dimension separation, proteins were transferred to a PVDF membrane (Hybond ECL, GE Healthcare) [25]. The membranes were stained with Ponceau Red (0.2% w/v Ponceau S in 3% v/v trichloroacetic acid) to check correct protein transfer and equal protein loading. Western blot analysis was performed using rabbit polyclonal antibodies anti-2,4-dinitrophenol (DNP) (Sigma, St. Louis, MO, USA; dilution 1:10000). The immunoreactive spots were detected using goat peroxidase-conjugated antirabbit immunoglobulin G (Sigma, working dilution 1:7000) and an ECL chemiluminescence detection system (GE Healthcare). Chemiluminescent signals were captured after different exposure times (3 min, 10 min, 20 min). The digital 2D western blot images were then analysed with Image Master Platinum 7.0 for semi-quantitative analysis using the relative integrated density values of the spots (spot intensity). Immunoblot data was then exported into Excel (Microsoft Office) and histograms of the oxidized spots in the three conditions (T0, T1M and T1B) were plotted.

3. Results

3.1. Clinical data

Table 1 reports the main characteristics of the population: demographic data, ACT score, eosinophil count, serum IgE and lung function parameters. No differences in demographic and baseline functional and immunological data were observed between groups.

Table 1
Demographic, clinical, immunological and functional parameters of study population at baseline.

Baseline characteristics	Mepolizumab treated patients ($n = 10$)	Benralizumab treated patients ($n = 8$)	*P* values
Age	56 ± 11	50.5 ± 16.1	ns
Gender (F/M)	2/8	4/4	ns
Smoking Habits (Former-current /never)	6/4	6/2	ns
Age at onset	33.2 ± 16.6	34.3 ± 17	ns
OCS dosage	3.7 ± 4.3	4 ± 4.5	ns
Eosinophil cell count (cell/mm3)	1090 ± 821	719 ± 419	ns
Eosinophil cell count (%)	11.6 ± 7	8.2 ± 4.6	ns
Functional parameters:			
• FEV1(%)	77 ± 27	81 ± 25	ns
• FVC	92 ± 21	99 ± 23	ns
• TIFFENAU index	66 ± 16	66 ± 8	ns
ACT Score	14 ± 6	a14.8 ± 6.8	ns

Oral corticosteroid dosage is expressed as prednisone-equivalent. OCS: oral corticosteroids; ACT: Asthma Control Test; ACQ: Asthma Control Questionnaire. Comparison of clinical questionnaires, eosinophil cell count and FEV1% before and after one month of treatment. *: comparison of Mepolizumab and Benralizumab groups.

After one month of therapy, all patients referred symptomatic improvement and abolition of the use of salbutamol at request and improved significantly in terms of functional and immunological parameters, as well as clinical status as reported in Table 2 [27].

3.2. Proteomic analysis

Our study compared serum protein patterns of ten patients with severe eosinophilic asthma before (T0) and after one month of treatment with Benralizumab (T1B 5 patients) or Mepolizumab (T1M 5 patients). We used 2DE to obtain specific gels showing typical serum protein patterns with an average of 1473 spots *per gel*. Comparative analysis highlighted 38 differences between T0, T1M and T1B profiles, visible in Fig. 1 and reported in Table S1. Table 3 shows the proteins identified by mass spectrometry. Fig. 2 shows two spots exclusive to T0, ten exclusives to T1B, five exclusives to T1M (reported in bold) and up-regulated protein species related to each group (T0, T1B, T1M).

3.3. PCA, t-SNE and heat map analysis

Unsupervised proteomic data from T0, T1M and T1B serum samples reported in Table S2, clustered separately when analysed by PCA and t-SNE (Fig. 3). In particular, Benralizumab and Mepolizumab samples were distant from T0 along the main component (PC1), and only one sample from the Mepolizumab group clustered with Benralizumab samples. The two treatments distinguished the samples along the second main component (PC2). T-SNE analysis highlighted the influence of different treatments on serum protein abundance, grouping our samples in three separate groups along t-SNE1.

Numerous ceruloplasmin protein species were found to be more abundant in T1B than in T0 samples, unlike in the case of T1M compared with T0 samples. PCA analysis of the differential ceruloplasmin spots showed that while T0 and Mepolizumab samples clustered near each other, Benralizumab clustered separately along PC1 (Fig. 3, ceruloplasmin).

Fig. 4 shows the results of heat map analysis of unsupervised proteomics data with the abundance trends of matched spots in all gels. Protein abundance was homogeneous in the T0 group, while it showed an opposite pattern in the T1M and T1B groups (particularly evident at the top of the map).

3.4. MetaCore analysis

Protein species up-regulated in T1B and T1M groups, visualized by Venn diagram, were uploaded separately to MetaCore to obtain protein networks specific for the two treatment groups. Fig. 5A shows the network of highly abundant proteins after one month of Benralizumab treatment; plasmin, alpha 1-antitrypsin (A1AT), plasminogen (PLMN) and alpha-2-macroglobulin (A2M) emerged as the functional hubs. Two canonical pathways emerged from this network, one involving the coagulation cascade and MAPK signalling activated by IL-1beta, modulating transcription factor AP-1 and inducing ceruloplasmin; the other involving the leptin receptor (LEPR) that positively regulates A2M release through the STAT3, STAT5A and STAT5B pathways.

Fig. 5B shows the network of proteins up-regulated after one month of Mepolizumab treatment, where A1AT, albumin (ALBU), fibrinogen gamma (FIBG), factor B (FIBB) and plasmin emerge as functional hubs. A canonical path concerned with haemostasis inhibited by A1AT was found (red arrows).

The principal biological processes related to Mepolizumab and Benralizumab treatments are compared in Fig. 5C. Defence response, complement activation, vesicle-mediated transport, immune effector process, immune response, endocytosis, response to stress, import into cell and leukocyte-mediated immunity were the most relevant biological processes involving up-regulated proteins after Mepolizumab treatment. On the other hand, platelet degranulation, acute phase response and exocytosis were the major processes related to Benralizumab treatment. Post-translational protein modification had the same statistical

Table 2
Functional, immunological, and serum analysis in patients at T0 and T1 in mepolizumab- and benralizumab-treated patients [27].

	Mepolizumab group			Benralizumab group		
	T0	T1	P values	T0	T1	P values
Functional parameters:						
• FEV1(%)	84,4 ± 26,6	87,1 ± 21,5	0,04	81,3 ± 25	89,7 ± 15	0,04
• FEV1(ml)	2558,86 ± 886	2820 ± 960,7	0,0037	2607,5 ± 1067,3	2747,1 ± 847,6	0,005
• TIFFENAU index	69,4 ± 12,4	72,8 ± 10,26	0,04	66 ± 8,4	70,5 ± 9	0,04
Peripheral eosinophilia (migl/mm3/%)	915 ± 617 / 11,4 ± 6,5	140 ± 83,5 / 1,6 ± 1,2	<0,0001	718 ± 49 / 8,2 ± 4,6	0 / 0	<0,0001
sL-selectin (ng/ml)	1442 ± 1003	630 ± 413	0,0012	1173 ± 683	1360,3 ± 1289	ns
KL-6 (U/ml)	332,7 ± 124	310,7 ± 107,1	ns	334,6 ± 76,8	329,1 ± 88,3	ns
Lymphocytes immunophenotyping:						
CD45	19,1 ± 5,4	17,9 ± 7,4	ns	24,5 ± 11,8	28,5 ± 1,3	ns
CD3	81,8 ± 8,5	79,5 ± 7,7	ns	81,6 ± 5	76 ± 6,7	ns
CD4	47,9 ± 12	53,5 ± 8,4	ns	58,5 ± 3,4	52 ± 10	ns
CD8	31,7 ± 14	24 ± 8	0,03	20,5 ± 8,6	22 ± 4,8	ns
CD19	7,8 ± 5,2	8,3 ± 5,7	ns	8,5 ± 3,1	10,7 ± 2	ns
NK	9,9 ± 5,8	13 ± 16	ns	10,7 ± 6,9	11,1 ± 3,4	ns
NKT-like	12,21 ± 8,7	8,4 ± 8,3	0,02	15,6 ± 23	15,1 ± 6	ns

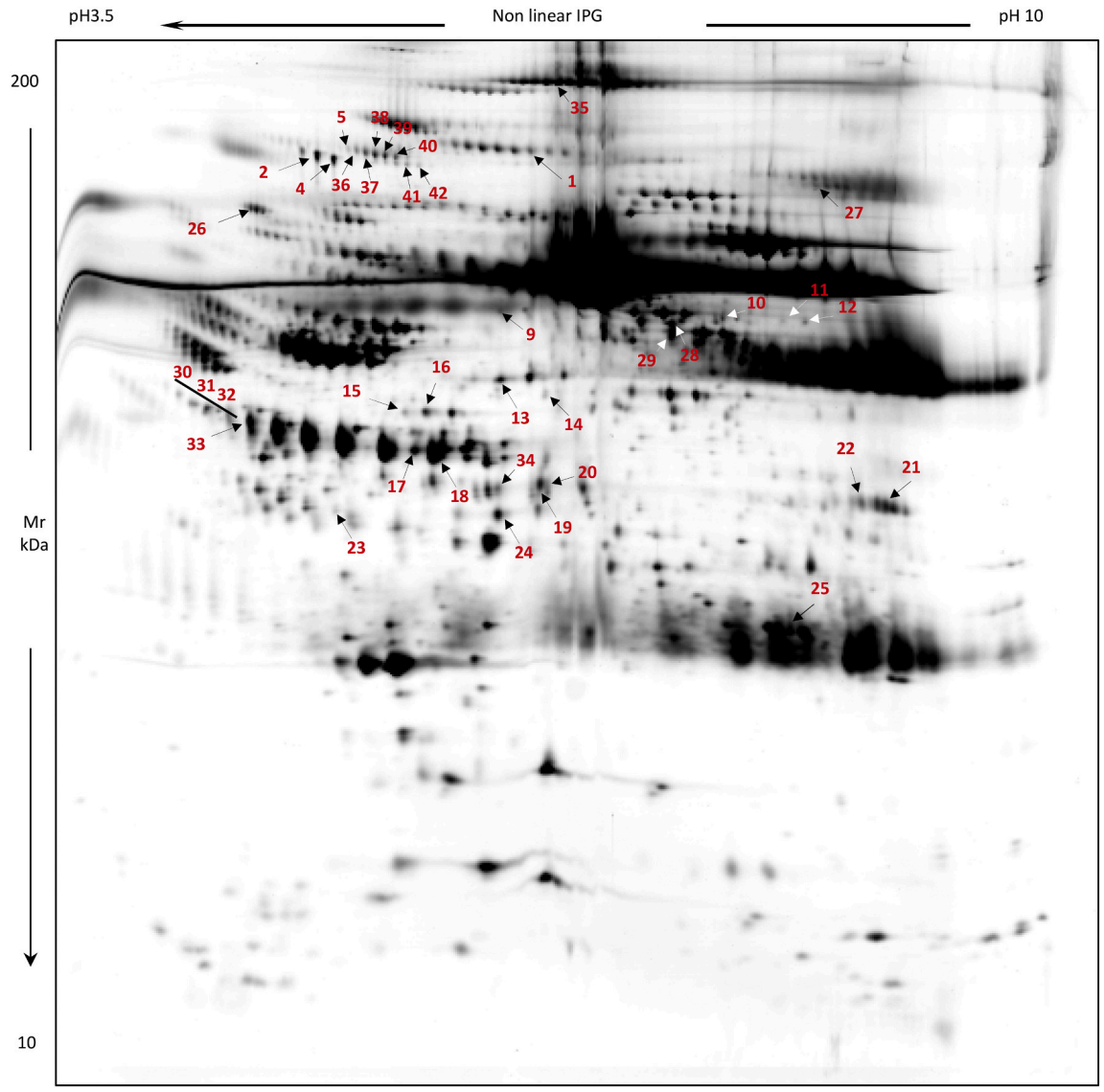


Fig. 1. Gel Master report of differential proteins in serum from patients before treatment (T0), serum from patients after one month of Benralizumab (T1B) and serum from patients after one month of Mepolizumab (T1M). Arrows indicate differential protein spots and the numbers correspond to those in Table 2.

significance in both treatment groups.

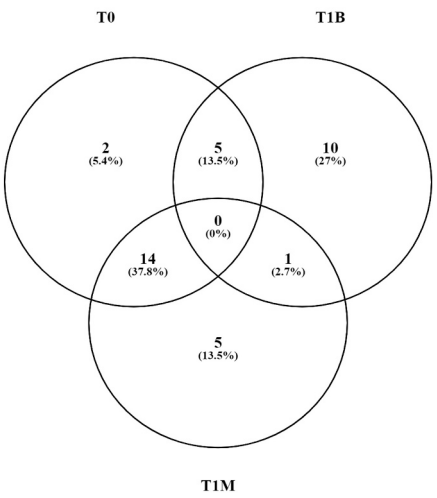
3.5. 1DE and 2DE western blot of ceruloplasmin

After one month of Benralizumab treatment (unlike after Mepolizumab), up-regulation of different ceruloplasmin protein species emerged in our proteomic analysis (Fig. 1: isoelectric series with spots 37, 38, 41, 42; Fig. S1), further highlighted by PCA. This potential biomarker was validated in a different population of patients. We performed 1DEWB comparing T1M *vs* T1B *vs* T0 *versus* healthy (control) serum samples. As shown in Fig. 6, 1DEWB highlighted two bands of ceruloplasmin. The abundance of the lower band of this protein in T1B (indicated by the arrow) and reported in the histograms, confirms our proteomic data that only showed differential spots in the lower isoelectric series of 2D-gels, as highlighted in Fig. S1.

To improve our analysis, all ceruloplasmin proteoforms were investigated by 2DEWB and the results are showed in Fig. 6. 2DEWBs not only highlighted the two isoelectric series of CERU with a strong signal, but also some spots with lower molecular weight (MW; indicated with arrows and letters) that are not detected in silver stained gels and with an interesting behavior. While these spots were clearly visible in control samples, they were absent in T0 and T1M samples. They reappeared after one month of Benralizumab treatment, more abundantly than in controls as shown by the histogram of intensities (control, T0, T1M and T1B). This behavior could be explained with an increase of the full-length ceruloplasmin, corresponding to an increase of its proteolityic products and so corroborating our results of an increase of ceruloplasmin after 1 month of Benralizumab treatment.

3.6. Redox proteomics

Oxidative stress has a pivotal role in the pathogenesis of severe asthma [28] and the abundant protein species of the antioxidant ceruloplasmin demonstrated by us in serum after one month of Benralizumab therapy prompted us to evaluate serum oxidized protein patterns before and after Mepolizumab and Benralizumab treatment. Fig. 7 shows 2DWB oxidized protein patterns in T0, T1M and T1B gels and the reference 2DE serum gel map. Three histograms were constructed on the basis of spot and isoelectric series intensity (Fig. 8). The first histogram (+OX T1B) showed two spots and two isoelectric series that were highly oxidized with respect to T0 and T1M after one month of Benralizumab treatment. The second histogram (+OX T0) showed eight spots and



T0	T1B	T1M
1.	2. A1AT	1.
5.CERU	**4. A1AT**	2.A1AT
9.IGHA1	5. CERU	9.IGHA1
10. ALBU	**26. C1S**	10. ALBU
11.FIBB	**27.PLMN**	12.FIBB
12.FIBB	**28. ALBU**	**13.FIBG**
14.	30. FETUA	14.
15. ALBU	31. FETUA	15. ALBU
17. ALBU	33.ZA2G	**16. ALBU**
18.ALBU	**34.**	17.ALBU
19.ALBU	35. A2MG	18.ALBU
20.	**36.**	19. ALBU
22.IGHG2	**37.CERU**	20.
23.	**38. CERU**	**21.**
25. IGL1	**41. CERU**	22.IGHG2
29.ALBU	**42.CERU**	23.
30.FETUA		**24.ALBU**
31. FETUA		25. IGL1
33. ZA2G		29.ALBU
35.A2MG		**32.FETUA**
40.		

Fig. 2. Venn's diagram with the number of up-regulated spots in and shared by T1B, T1M and T0 serum. Differential protein species are reported in Table referred to the diagram. Up-regulated proteins unique to T1B, T1M and T0 serum are indicated in bold.

three isoelectric series that were highly oxidized before treatment and the third histogram (+OX T1M) showed 17 spots and 12 isoelectric series highly oxidized with respect to T1B and T0 after one month of Mepolizumab treatment. These results showed that after one month of Mepolizumab, higher oxidative burst was observed than after one month of Benralizumab and in pre-treatment serum. Benralizumab treatment determined lower levels of serum oxidation.

4. Discussion

In the present study, proteomic profiles of serum samples from patients with severe asthma were evaluated before and after treatment with Mepolizumab or Benralizumab. Intriguingly, different protein abundance trends were observed in the two treatment groups, although the two drugs have similar targets. We demonstrated by enrichment analysis that Mepolizumab determined increased abundance of proteins relevant to the pathogenesis of asthma, modulating defence response, complement activation, vesicle-mediated transport, immune response, endocytosis, stress-responses, leukocyte-mediated immunity and post-translational protein modification. The major players in these processes were A1AT, ALBU, FIBG, FIBB and plasmin. In particular, the up-regulation of A1AT protein species found by us was related to the coagulation cascade in the network inhibiting thrombin and plasmin, in line with the results of Churg et al. [29]. Talens et al. also reported A1AT strongly associated with fibrin clots, representing a link between inflammatory and haemostatic systems regulating proteases involved in coagulation or fibrinolysis [30]. By proteomics, we also found a higher molecular weight proteoform of A1AT in polymer form, in line with Quinn et al., who reported polymeric A1AT complexed with IgE, involved in the pathophysiology of lung diseases, that arise either as a consequence of A1AT-deficiency or through IgE-mediated hypersensitivity responses [31].

We found that Mepolizumab treatment determined an up-regulation of various protein species of albumin. In the network, albumin was associated with the neonatal Fc receptor (FcRn), expression of which can

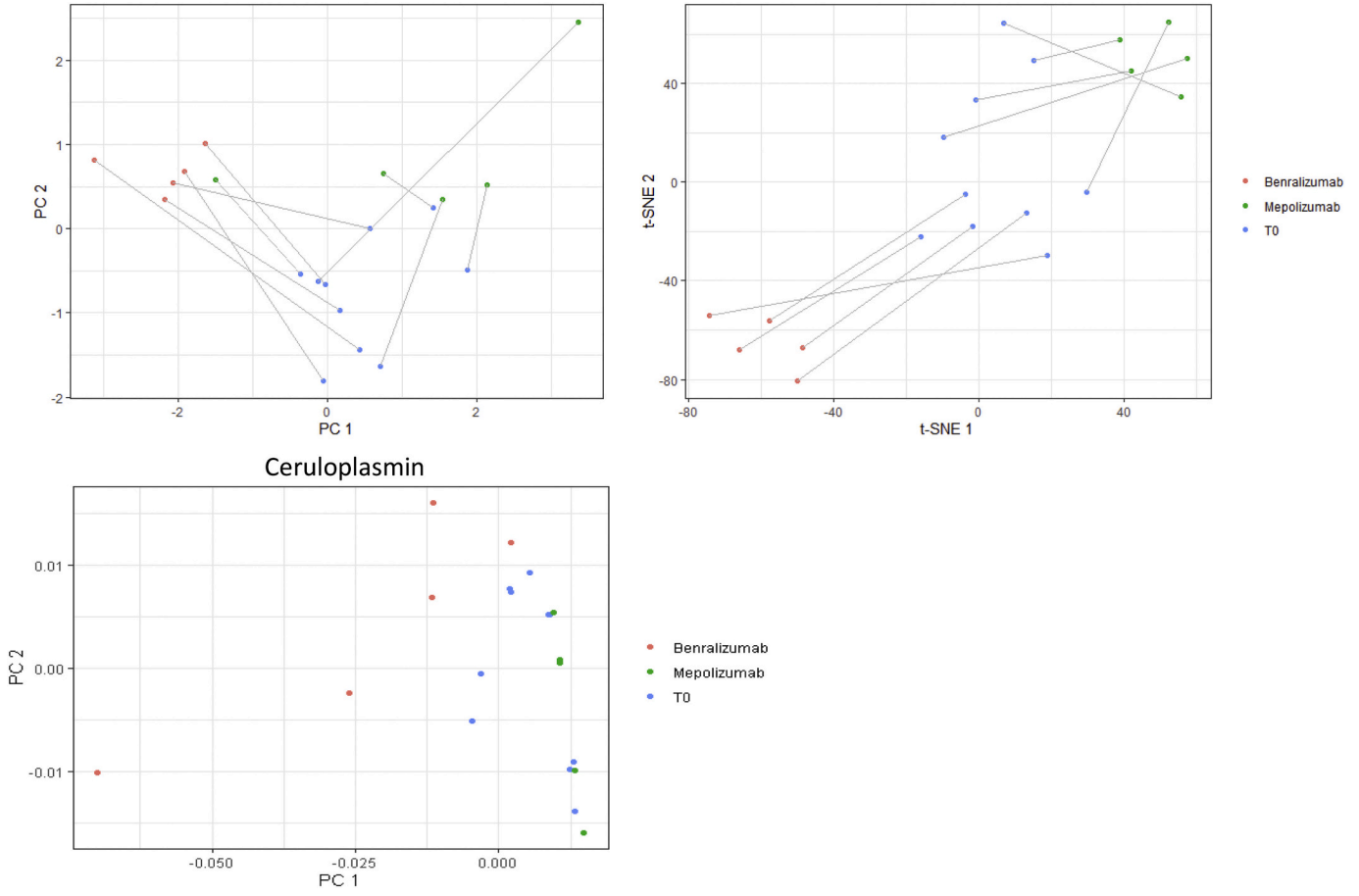


Fig. 3. Principal Component Analysis (PCA) and t-SNE analysis (t-SNE) performed with unsupervised proteomic data. PCA performed with the differential spots of ceruloplasmin.

Table 3
Protein identification by mass spectrometry, showing spot numbers corresponding to Fig. 1 and Table S1, protein names, UniProt names and accession number, theoretical and experimental p*I* and MW and Mascot Search Results (Score, Matched peptides, Coverage%).

Spot Number	Protein Name	UniProt Name	UniProt AC	Theorethical pI/MW	Experimental pI/MW	Score	Matched Peptides	Coverage %
2	Alpha-1-antitrypsin	A1AT	P01009	5.3746707	5.30110210	213	19	48
4	Alpha-1-antitrypsin	A1AT	P01009	5.3746707	5.32110207	223	18	48
5	Ceruloplasmin	CERU	P00450	5.44122127	5.08110472	9	11	120
9	Immunoglobulin heavy constant alpha 1	IGHA1	P01876	6.0838486	5.9958094	68	12	29
10	Serum albumin	ALBU	P02768	5.9269321	6.0557487	100	9	18
11	Complement Factor B	FIBB	P00751	6.67 86.85	6.4557341	135	14	21
12	Complement Factor B	FIBB	P00751	6.67 86.85	6.4957339	131	18	37
13	Fibrinogen gamma chain	FIBG	P02679	5.3751478	5.8954978	173	17	48
15	Serum Albumin	ALBU	P02768	5.92 71.32	5.5653843	125	13	22
16	Serum Albumin	ALBU	P02768	5.92 71.32	5.5953842	115	14	22
17	Serum Albumin	ALBU	P02768	5.9247098	5.2641833	165	54	71
18	Serum albumin	ALBU	P02768	5.92 71.32	5.6451204	100	9	12
19	Albumin C-term	ALBU	P02768	5.92 71.32	5.6538626	92	6	11
22	Immunoglobulin heavy constant gamma 2	IGHG2	P01859	7.6636505	7.0438318	54	16	46
24	Serum albumin	ALBU	P02768	5.92 71.32	5.6450108	103	10	15
25	Immunoglobulin lambda-1 light chain OS	IGL1	P15814	6.3423101	6.7424587	32	9	47
26	Complement C1s subcomponent	C1S	P09871	4.8678174	4.7998509	72	34	43
27	Plasminogen	PLMN	P00747	7.0493247	7.5392846	223	52	58
28	Serum Albumin	ALBU	P02768	5.92 71.32	6.0957488	122	13	21
29	Serum Albumin	ALBU	P02768	5.92 71.32	6.1056759	117	12	19
30	Alpha-2-HS-glycoprotein	FETUA	P02765	5.4339341	4.6057929	HTLNQIDEVK FSVVYAK CNLLAEK EHAVEGDCDFQLLK HTFMGVVSLGSPSGEVSHPR		
31	Alpha-2-HS-glycoprotein	FETUA	P02765	5.4339341	4.6156039	HTLNQIDEVK EHAVEGDCDFQLLK		
32	Alpha-2-HS-glycoprotein	FETUA	P02765	5.4339341	4.5855367	73	5	18
33	Zinc-alpha-2-glycoprotein	ZA2G	P25311	5.7134237	4.9734192	127	12	43
35	Alpha-2-macroglobulin	A2MG	P01023	6.03164613	5.56199953	41	74	46
37	Ceruloplasmin	CERU	P00450	5.44122127	5.11133671	92	7	8
38	Ceruloplasmin	CERU	P00450	5.44122127	5.13133671	105	8	10
41	Ceruloplasmin	CERU	P00450	5.44122127	5.15131456	126	12	18
42	Ceruloplasmin	CERU	P00450	5.44122127	5.21129128	126	12	16

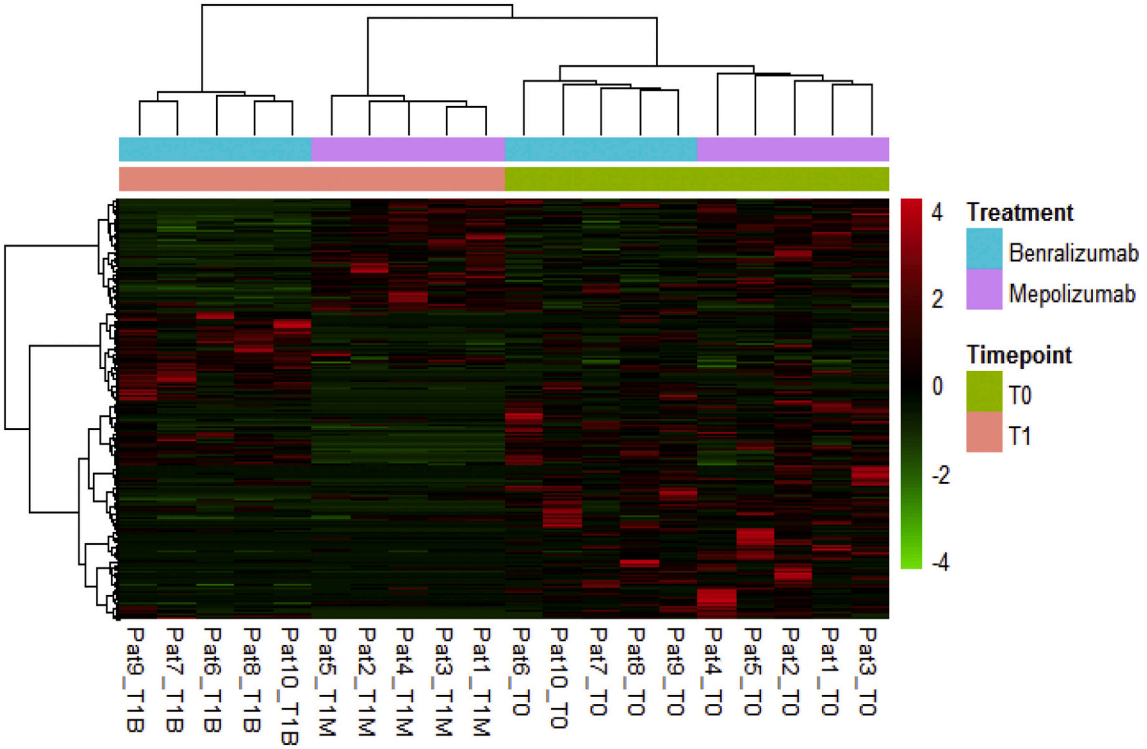


Fig. 4. Heat map analysis performed with unsupervised proteomic data. Colour change from red to green indicating greater or less protein abundance, respectively.

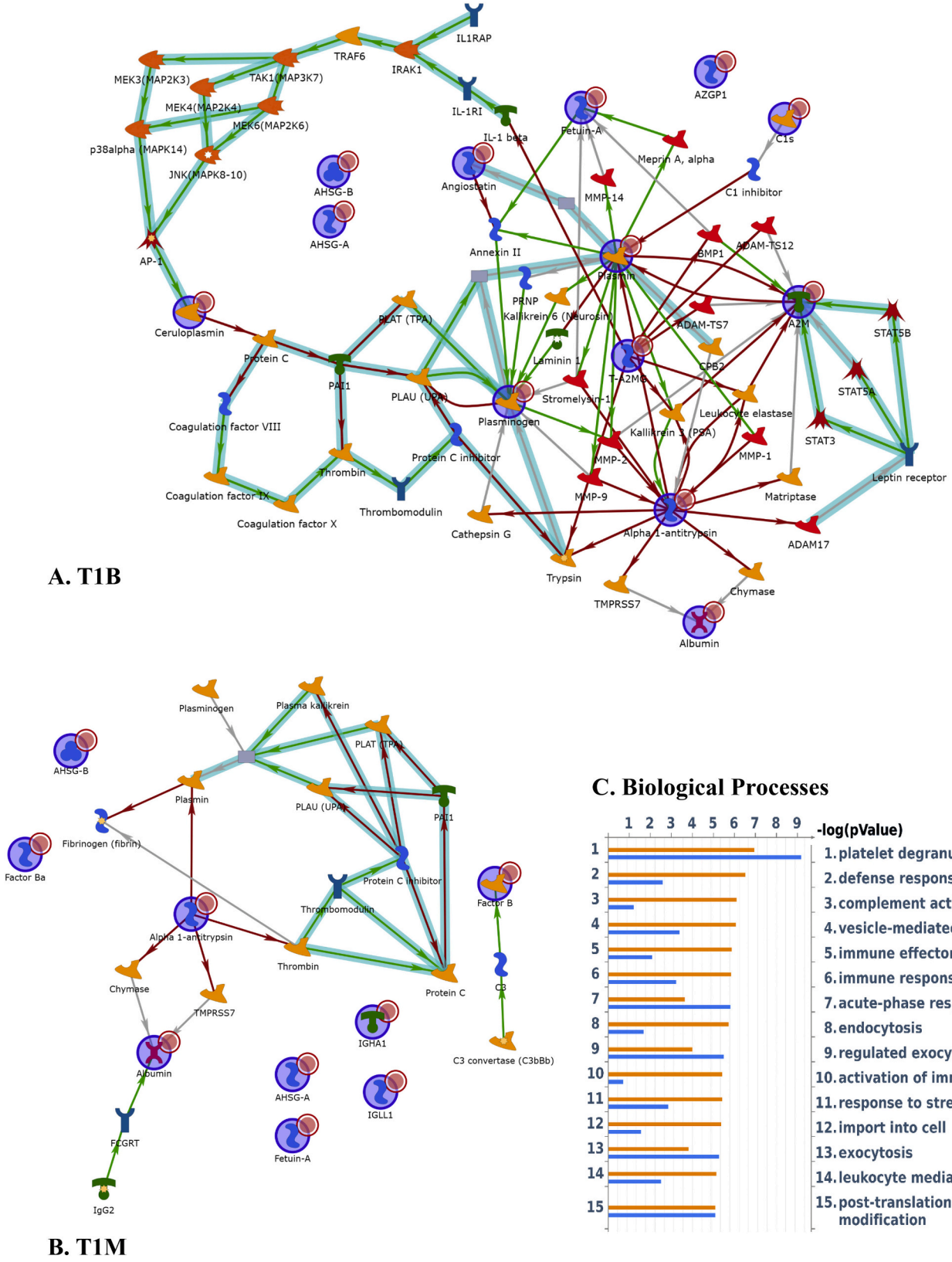
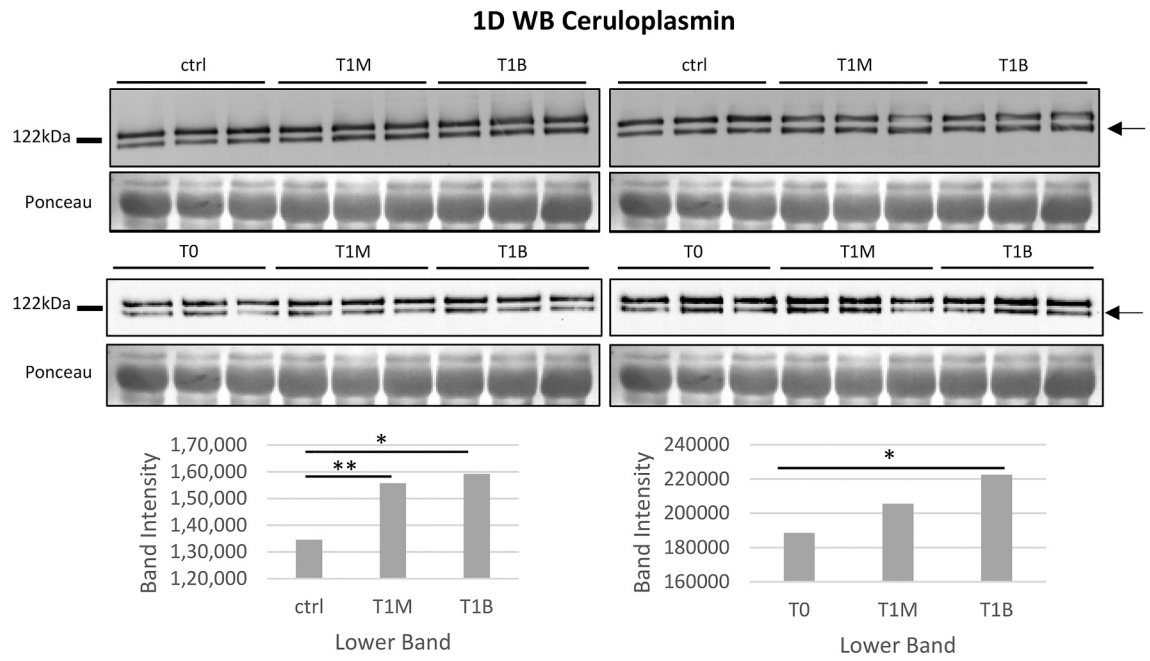


Fig. 5. MetaCore Analysis: A. proteins up-regulated in T1B serum. B. proteins up-regulated in T1M serum. C. Comparison of biological processes by gene ontology of up-regulated proteins in T1B and T1M serum. Orange histograms show T1M proteins; blue histograms show T1B proteins.



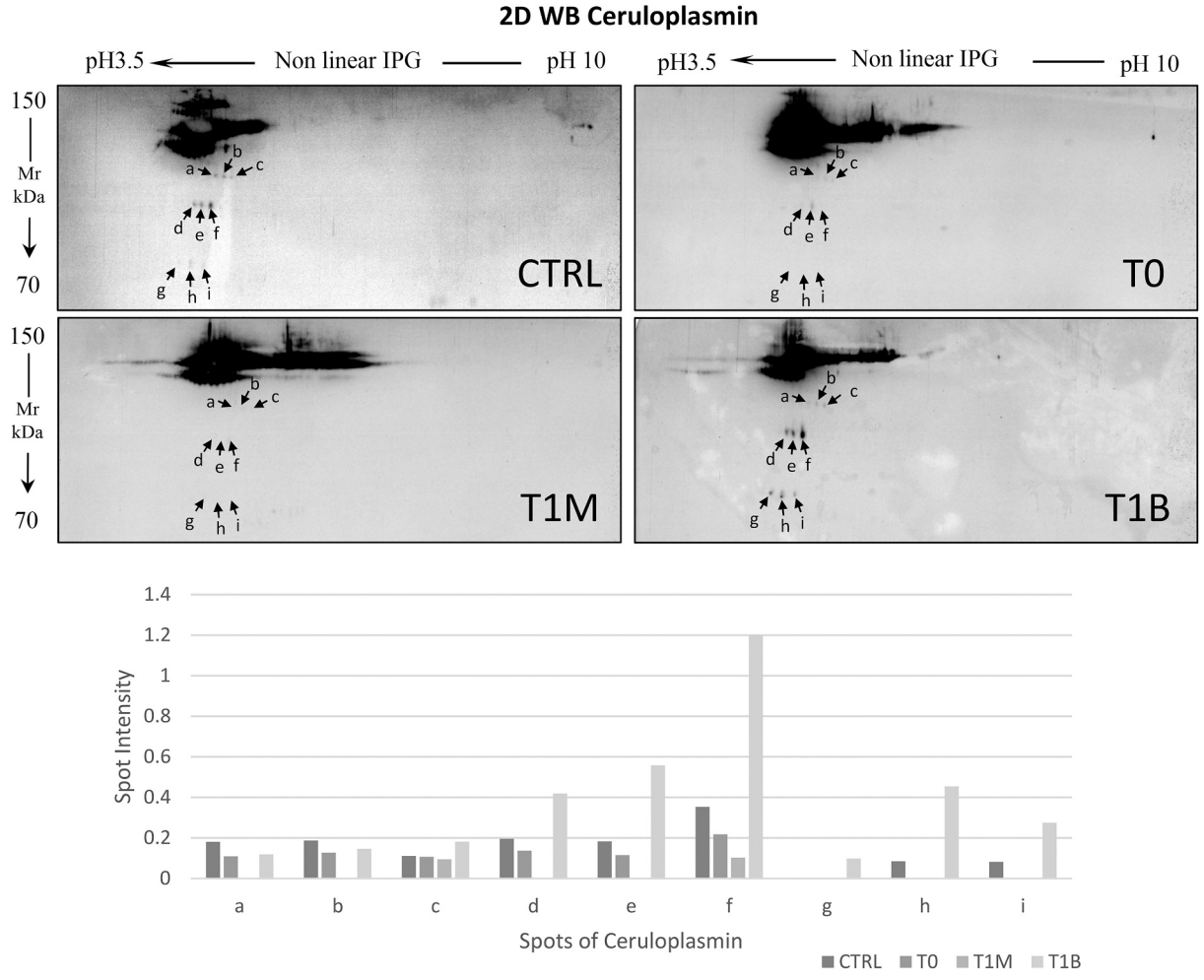


Fig. 6. 1DEWB: One-dimensional western blot of ceruloplasmin. The lower band validates up-regulation of ceruloplasmin in T1B serum. * $p < 0.05$, ** $p < 0.01$. 2DEWB: Two-dimensional western blot of ceruloplasmin. Arrows and letters show differential ceruloplasmin spots between Control, T0, T1M and T1B serum. Histogram shows spot intensities in T1B, T1M and T0 serum.

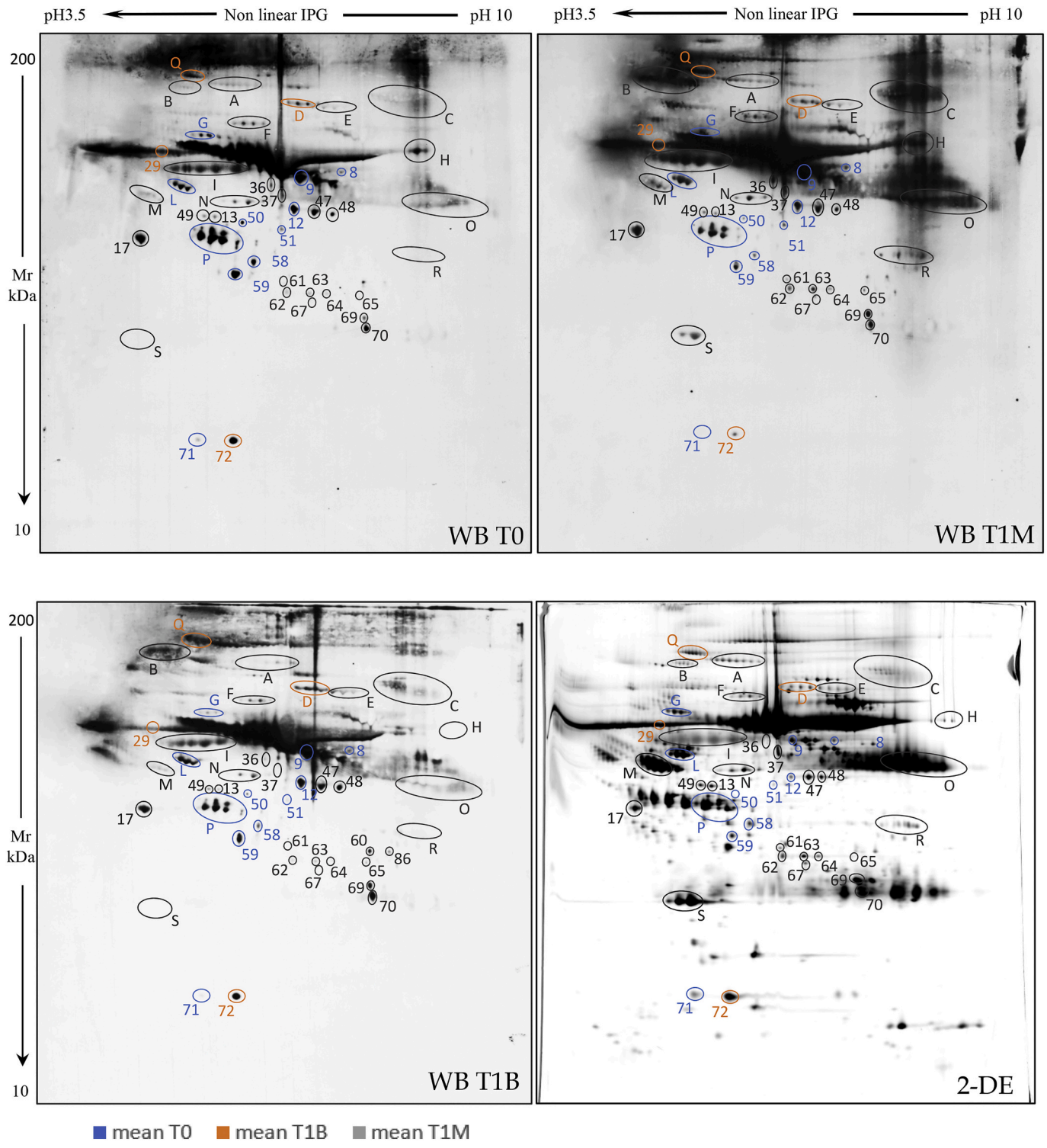


Fig. 7. Redox profile of T0, T1M, T1B serum samples and reference silver-stained 2-DE gels. Blue circles highlight highly oxidized spots in T0 serum, orange circles highly oxidized spots in T1B and grey circles highly oxidized spots in T1M serum.

be modulated by the immunological context, suggesting a possible Mepolizumab-mediated effect. FcRn regulates systemic IgG and albumin homeostasis, binding these proteins at acid pH, characteristic of early and late endosomes and potentially of the extracellular milieu associated with inflammation [32]. Curiously, different proteoforms of immunoglobulins such as IGHA and IGL1 were also up-regulated after Mepolizumab therapy.

On the other hand, Benralizumab administration determined up-regulation of proteins involved in platelet degranulation, acute-phase response, regulated exocytosis and post-translational protein modifications. Plasmin, A1AT, PLMN and A2M played a central functional role in these mechanisms. Interestingly, several ceruloplasmin proteoforms increased in abundance only in patients treated with Benralizumab, suggesting that ceruloplasmin (CERU) is a protein expressed differentially in these two biological therapies. Plasma levels of CERU are normally increased in response to inflammation [33,34] and the network

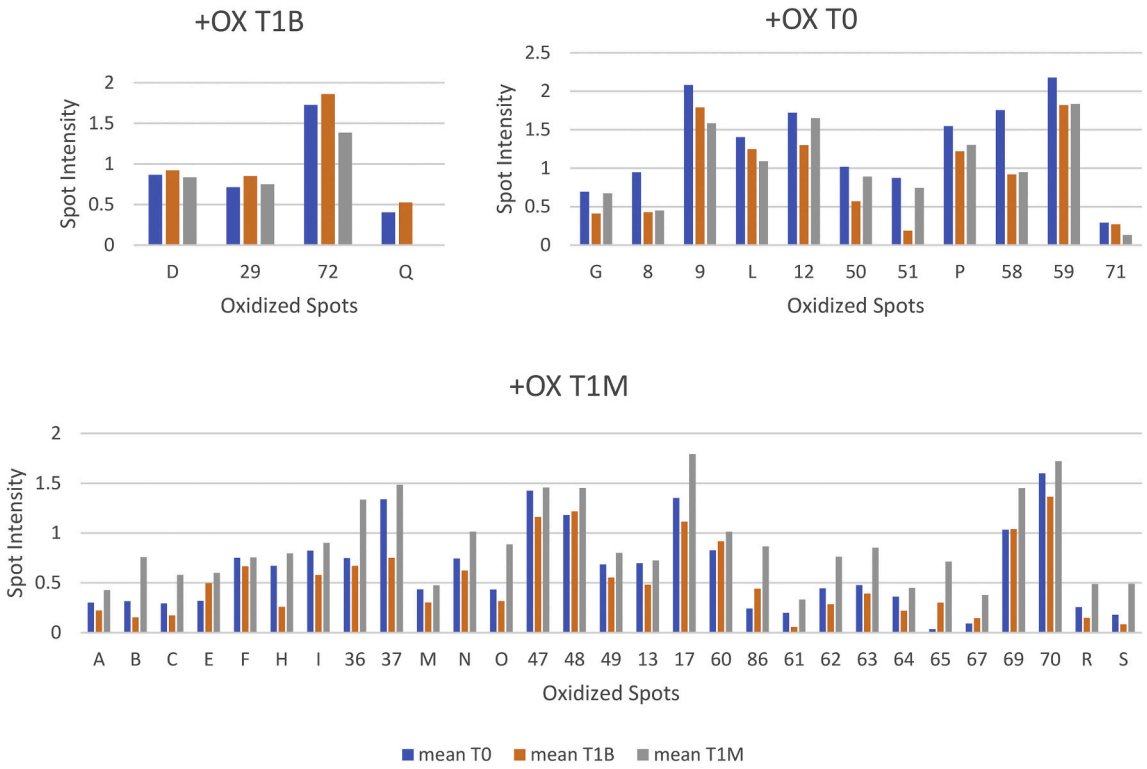


Fig. 8. Histograms reporting levels of oxidation for each spots or isoelectric series in T1B, T0 and T1M 2DWB.

indicates that CERU inhibits protein C, a potent inhibitor of blood coagulation [33]. Benralizumab treatment may act on this specific pathway of the coagulation cascade and indeed in our study, high abundance of PLMN was observed. Ceruloplasmin is a ferroxidase enzyme, synthesized by the liver and various non-hepatic tissues, including the lungs. It is able to inhibit lipid peroxidation and the Fenton reaction, acting as a circulating scavenger of superoxide anion radicals and protecting cells and tissues against the detrimental effects of free radicals [35]. Ceruloplasmin is regulated by a copper-dependent transcriptional mechanism requiring an AP-1 responsive element [36], as shown in the MetaCore network. In turn, AP-1 is regulated by a p38 MAPK-dependent mechanism, activated by IL-1 [37], availability of which is regulated by haemostasis processes [38] and inflammatory responses [39]. In particular, our protein network suggested that IL-1 was regulated by A2M, a cytokine transporter and protease inhibitor of trypsin, thrombin and collagenase. Interestingly, A2M release may also be determined through the STAT3, STAT5A and STAT5B pathways by the leptin receptor (LEPR), suggested by MetaCore. LEPR is involved in PI3K, MAPK and JAK-STAT signalling pathways and has been reported to be down-regulated in severe asthmatics carrying evidence of airway remodelling [40].

The rising levels of serum CERU reported in patients after one month of treatment with Benralizumab may indicate high cell stress with greater ferroxidase activity in response to this treatment. An alternative hypothesis is that the increased concentrations of CERU may be expression of a lowering of asthma-induced oxidative stress mediated by the anti-inflammatory biological treatment [41].

Different authors have investigated the effects of ceruloplasmin administration in combination with conventional treatments in asthma patients, reporting a reduction of ROS generation in blood and improvement in respiratory symptoms with respect to patients treated with conventional therapies alone [42,43]. This prompted us to perform redox proteomics which revealed oxidized protein patterns in serum samples drawn before and after one month of the two treatments. Highly oxidized spots or isoelectric series were mainly found in serum of patients treated with Mepolizumab, suggesting high oxidative stress in these subjects. Serum from patients treated with Benralizumab showed fewer oxidized spots and isoelectric series than serum form the Mepolizumab group, corroborating our hypothesis that high ceruloplasmin levels protect against oxidative stress induced by severe asthma.

The limits of the present study include the short follow-up and small study population.

5. Conclusions

Mepolizumab and Benralizumab are two current biological treatments for severe eosinophilic asthma. Clinicians have no biomarkers to distinguish which of the two is the more suitable for a given patient or to verify response to treatment [44]. Our proteomic analysis highlighted differential protein profiles associated with each biological therapy, in particular ceruloplasmin and oxidative serum proteins. An aim of further research will be to clarify the relationship between Th2 inflammation and the coagulation cascade in patients on biological therapies, and to validate these results in long term follow-up.

Supplementary data to this article can be found online at https://doi.org/10.1016/j.bbapap.2020.140563.

Author contributions

All authors had full access to all the data of the study and took responsibility for the integrity of the data and the accuracy of the data analysis. Conceptualization, EB, CL, PC; Methodology, LB, Md, FdG, SA; Investigation, LV, AC, LB; Formal Analysis, CL, LV, AC, PC, ES; Writing CL, EB; Writing – Review & Editing, EB, LBini.

Data availability statement

Requests for further information about resources, reagents and data availability should be directed to the corresponding author.

Declaration of Competing Interest

The authors declare that they have no current or potential conflict of interest regarding this article.

Acknowledgments

Authors are grateful to Ms. Helen Ampt for careful English revision.

References

[1] D. Bagnasco, M. Ferrando, G. Varricchi, F. Puggioni, G. Passalacqua, G. W. Canonica, Anti-interleukin 5 (IL-5) and IL-5Ra biological drugs: efficacy, safety, and future perspectives in severe Eosinophilic asthma, Front. Med. (Lausanne). 4 (2017) 135.
[2] J.P. Abonia, P.E. Putnam, Mepolizumab in eosinophilic disorders, Expert. Rev. Clin. Immunol. 7 (4) (2011 Jul) 411–417.
[3] A. Ghazi, A. Trikha, W.J. Calhoun, Benralizumab–a humanized mAb to IL-5Rα with enhanced antibody-dependent cell-mediated cytotoxicity–a novel approach for the treatment of asthma, Expert. Opin. Biol. Ther. 12 (1) (2012 Jan) 113–118.
[4] M. Laviolette, D.L. Gossage, G. Gauvreau, R. Leigh, R. Olivenstein, R. Katial, et al., Effects of benralizumab on airway eosinophils in asthmatic patients with sputum eosinophilia, J. Allergy Clin. Immunol. 132 (5) (2013 Nov) 1086–1096.e5.
[5] P. Haldar, C.E. Brightling, B. Hargadon, S. Gupta, W. Monteiro, A. Sousa, et al., Mepolizumab and exacerbations of refractory eosinophilic asthma, N. Engl. J. Med. 360 (10) (2009 Mar 5) 973–984.
[6] I.D. Pavord, S. Korn, P. Howarth, E.R. Bleecker, R. Buhl, O.N. Keene, et al., Mepolizumab for severe eosinophilic asthma (DREAM): a multicentre, double-blind, placebo-controlled trial, Lancet. 380 (9842) (2012 Aug 18) 651–659.
[7] E.H. Bel, S.E. Wenzel, P.J. Thompson, C.M. Prazma, O.N. Keene, S.W. Yancey, et al., Oral glucocorticoid-sparing effect of mepolizumab in eosinophilic asthma, N. Engl. J. Med. 371 (13) (2014 Sep 25) 1189–1197.
[8] E.H. Bel, H.G. Ortega, I.D. Pavord, Glucocorticoids and mepolizumab in eosinophilic asthma, N Engl. J. Med. 371 (25) (2014) 18 (2434).
[9] H.G. Ortega, M.C. Liu, I.D. Pavord, G.G. Brusselle, J.M. FitzGerald, A. Chetta, et al., Mepolizumab treatment in patients with severe eosinophilic asthma, N. Engl. J. Med. 371 (13) (2014 Sep 25) 1198–1207.
[10] G.L. Chupp, E.S. Bradford, F.C. Albers, D.J. Bratton, J. Wang-Jairaj, L.M. Nelsen, et al., Efficacy of mepolizumab add-on therapy on health-related quality of life and markers of asthma control in severe eosinophilic asthma (MUSCA): a randomised, double-blind, placebo-controlled, parallel-group, multicentre, phase 3b trial, Lancet Respir. Med. 5 (5) (2017) 390–400.
[11] M. Castro, S.E. Wenzel, E.R. Bleecker, E. Pizzichini, P. Kuna, W.W. Busse, et al., Benralizumab, an anti-interleukin 5 receptor α monoclonal antibody, versus placebo for uncontrolled eosinophilic asthma: a phase 2b randomised dose-ranging study, Lancet Respir. Med. 2 (11) (2014 Nov) 879–890.
[12] R.M. Nowak, J.M. Parker, R.A. Silverman, B.H. Rowe, H. Smithline, F. Khan, et al., A randomized trial of benralizumab, an antiinterleukin 5 receptor α monoclonal antibody, after acute asthma, Am. J. Emerg. Med. 33 (1) (2015 Jan) 14–20.
[13] E.R. Bleecker, J.M. FitzGerald, P. Chanez, A. Papi, S.F. Weinstein, P. Barker, et al., Efficacy and safety of benralizumab for patients with severe asthma uncontrolled with high-dosage inhaled corticosteroids and long-acting β2-agonists (SIROCCO): a randomised, multicentre, placebo-controlled phase 3 trial, Lancet 388 (10056) (2016) 2115–2127, 29.
[14] J.M. FitzGerald, E.R. Bleecker, P. Nair, S. Korn, K. Ohta, M. Lommatzsch, et al., Benralizumab, an anti-interleukin-5 receptor α monoclonal antibody, as add-on treatment for patients with severe, uncontrolled, eosinophilic asthma (CALIMA): a randomised, double-blind, placebo-controlled phase 3 trial, Lancet 388 (10056) (2016) 2128–2141, 29.
[15] C.A. Akdis, Z.K. Ballas, Precision medicine and precision health: building blocks to foster a revolutionary health care model, J. Allergy Clin. Immunol. 137 (5) (2016) 1359–1361.
[16] M. Ferrando, D. Bagnasco, G. Varricchi, S. Bernardi, A. Bragantini, G. Passalacqua, et al., Personalized medicine in allergy, Allergy, Asthma Immunol. Res. 9 (1) (2017 Jan) 15–24.
[17] K.F. Chung, S.E. Wenzel, J.L. Brozek, A. Bush, M. Castro, P.J. Sterk, et al., International ERS/ATS guidelines on definition, evaluation and treatment of severe asthma, Eur. Respir. J. 43 (2) (2014 Feb 1) 343–373.
[18] B. Bjellqvist, C. Pasquali, F. Ravier, J.C. Sanchez, D. Hochstrasser, A nonlinear wide-range immobilized pH gradient for two-dimensional electrophoresis and its definition in a relevant pH scale, Electrophoresis. 14 (12) (1993 Dec) 1357–1365.
[19] C. Landi, E. Bargagli, A. Carleo, R.M. Refini, D. Bennett, L. Bianchi, et al., Bronchoalveolar lavage proteomic analysis in pulmonary fibrosis associated with systemic sclerosis: S100A6 and 14-3-3ε as potential biomarkers, Rheumatology (Oxford) 58 (1) (2019 Jan 1) 165–178.
[20] D.F. Hochstrasser, M.G. Harrington, A.C. Hochstrasser, M.J. Miller, C.R. Merril, Methods for increasing the resolution of two-dimensional protein electrophoresis, Anal. Biochem. 173 (2) (1988 Sep) 424–435.
[21] B.R. Oakley, D.R. Kirsch, N.R. Morris, A simplified ultrasensitive silver stain for detecting proteins in polyacrylamide gels, Anal. Biochem. 105 (2) (1980 Jul 1) 361–363.
[22] T. Rabilloud, Silver staining of 2D electrophoresis gels, Methods Mol. Biol. 893 (2012) 61–73.
[23] M. Sulpizio, S. Falone, F. Amicarelli, M. Marchisio, F. Di Giuseppe, E. Eleuterio, et al., Molecular basis underlying the biological effects elicited by extremely low-frequency magnetic field (ELF-MF) on neuroblastoma cells, J. Cell. Biochem. 112 (12) (2011 Dec) 3797–3806.
[24] UniProtKB/Swiss-Prot 2020_01 [Internet] [cited 2020 Apr 22]. Available from: https://www.uniprot.org/statistics/Swiss-Prot.
[25] H. Towbin, O. Ozbey, O. Zingel, An immunoblotting method for high-resolution isoelectric focusing of protein isoforms on immobilized pH gradients, Electrophoresis. 22 (10) (2001 Jun) 1887–1893.
[26] P. Rottoli, B. Magi, R. Cianti, E. Bargagli, C. Vagaggini, N. Nikiforakis, et al., Carbonylated proteins in bronchoalveolar lavage of patients with sarcoidosis, pulmonary fibrosis associated with systemic sclerosis and idiopathic pulmonary fibrosis, Proteomics. 5 (10) (2005 Jul) 2612–2618.
[27] L. Bergantini, M. d'Alessandro, P. Cameli, F. Bianchi, P. Sestini, E. Bargagli, et al., Personalized approach of severe Eosinophilic asthma patients treated with Mepolizumab and Benralizumab, Int. Arch. Allergy Immunol. (2020 Jul 30) 1–8.
[28] S.D. Brown, K.M. Baxter, S.T. Stephenson, A.M. Esper, L.A.S. Brown, A. M. Fitzpatrick, Airway TGF-β1 and oxidant stress in children with severe asthma: association with airflow limitation, J. Allergy Clin. Immunol. 129 (2) (2012 Feb) 388–396 (396.e1-8).
[29] A. Churg, X. Wang, R.D. Wang, S.C. Meixner, E.L.G. Pryzdial, Wright J.L. Alpha1-antitrypsin suppresses TNF-alpha, macrophages. MMP-12 production by cigarette smoke-stimulated, Am. J. Respir. Cell Mol. Biol. 37 (2) (2007 Aug) 144–151.
[30] S. Talens, J.J.M.C. Malfliet, P.T.W. van Hal, F.W.G. Leebeek, D.C. Rijken, Identification and characterization of α1 -antitrypsin in fibrin clots, J. Thromb. Haemost. 11 (7) (2013 Jul) 1319–1328.
[31] P.M. Quinn, D.W. Dunne, S.C. Moore, R.J. Pleass, IgE-tailpiece associates with α-1-antitrypsin (A1AT) to protect IgE from proteolysis without compromising its ability to interact with FcεRI, Sci. Rep. 6 (2016 Feb 4), 20509.
[32] M. Pyzik, T. Rath, W.I. Lencer, K. Baker, R.S. Blumberg, FcRn: the architect behind the immune and nonimmune functions of IgG and albumin, J. Immunol. 194 (10) (2015 May 15) 4595–4603.
[33] F.J. Walker, P.J. Fay, Characterization of an interaction between protein C and ceruloplasmin, J. Biol. Chem. 265 (4) (1990 Feb 5) 1834–1836.
[34] M.C.H. de Visser, J.H.M. Souverijn, F.R. Rosendaal, R.M. Bertina, The effect of plasma caeruloplasmin levels on the sensitivity for activated protein C, Br. J. Haematol. 118 (3) (2002 Sep) 843–846.
[35] I.M. Goldstein, H.B. Kaplan, H.S. Edelson, G. Weissmann, Ceruloplasmin. A scavenger of superoxide anion radicals, J. Biol. Chem. 254 (10) (1979 May 25) 4040–4045.
[36] D. Das, N. Tapryal, S.K. Goswami, P.L. Fox, C.K. Mukhopadhyay, Regulation of ceruloplasmin in human hepatic cells by redox active copper: identification of a novel AP-1 site in the ceruloplasmin gene, Biochem. J. 402 (1) (2007 Feb 15) 135–141.
[37] T. Persichini, N. Maio, M.C.B. di Patti, G. Rizzo, M. Colasanti, G. Musci, Interleukin-1β induces ceruloplasmin and ferroportin-1 gene expression via MAP kinases and C/EBPβ, AP-1, and NF-κB activation, Neurosci. Lett. 484 (2) (2010 Oct 29) 133–138.
[38] J.W. Weisel, Fibrinogen and fibrin, Adv. Protein Chem. 70 (2005) 247–299.
[39] Y. Ito, N. Kaneko, T. Iwasaki, S. Morikawa, K. Kaneko, J. Masumoto, IL-1 as a target in inflammation, Endocr Metab Immune Disord Drug Targets 15 (3) (2015) 206–211.
[40] A. Bruno, E. Pace, P. Chanez, D. Gras, I. Vachier, G. Chiappara, et al., Leptin and leptin receptor expression in asthma, J. Allergy Clin. Immunol. 124 (2) (2009 Aug) 230–237 (237.e1-4).
[41] V. Mishra, J. Banga, P. Silveyra, Oxidative stress and cellular pathways of asthma and inflammation: therapeutic strategies and pharmacological targets, Pharmacol. Ther. 181 (2018) 169–182.
[42] U.R. Farkhutdinov, S.U. Farkhutdinov, Efficacy of ceruloplasmin in patients with asthma, Ter. Arkh. 84 (12) (2012) 45–48.
[43] V.M. Provotorov, A.V. Budnevsky, Y.I. Filatova, Clinical manifestations of asthma during combination therapy using ceruloplasmin, Ter. Arkh. 88 (3) (2016) 36–39.
[44] L. Bergantini, P. Cameli, M. d'Alessandro, L. Vietri, M. Perruzza, M. Pieroni, et al., Regulatory T cells in severe persistent asthma in the era of monoclonal antibodies target therapies, Inflammation. 43 (2) (2020 Apr) 393–400.
[45] Lorenza Vantaggiato, et al., Mepolizumab and Benralizumab in Severe Eosinophilic Asthma: Preliminary Results of a Proteomic Study, Lung 5 (198) (2020) 761–765, https://doi.org/10.1007/s00408-020-00379-6.